THE UNIVERSITY OF WESTERN AUSTRALIA

Research Report of Intelligent Systems for Medicine Laboratory

Report # ISML/02/2017, February 2017

A simple and effective method of incorporating the effects of residual stress in the abdominal aortic aneurysm wall stress estimation

Grand Roman Joldes[1], Christopher Noble[2], Stanislav Polzer[3], Zeike A Taylor[2], Adam Wittek[1], Karol Miller[1]

[1]Intelligent Systems for Medicine Laboratory
School of Mechanical Engineering
The University of Western Australia
35 Stirling Highway
Crawley WA 6009, AUSTRALIA
Phone: + (61) 8 6488 1901
Fax: + (61) 8 6488 1024
Email: grand.joldes@uwa.edu.au
http://school.mech.uwa.edu.au/ISML

[2]CISTIB, Centre for Computational Imaging and Simulation Technologies in Biomedicine, INSIGNEO Institute for in silico Medicine, Department of Mechanical Engineering, The University of Sheffield, Sheffield, UK

[3]Institute of Solid Mechanics, Mechatronics and Biomechanics, Brno University of Technology, Czech Republic

Abstract

Residual stress has a great influence on the mechanical behaviour of arterial walls. The Uniform Stress Hypothesis has been used to allow the inclusion of the effects of residual stress when computing stress distributions in the arterial wall of abdominal aortic aneurysms. Nevertheless, the existing methods for including the effects of residual stress are very computationally expensive, due to their iterative nature.

In this paper we present a new method for including the effects of residual stress. Also based on the Uniform Stress Hypothesis, the new method is based on the averaging of stresses across the thickness of the arterial wall. Being just a post-processing method for computed stress distributions, the new method is computationally inexpensive, being better suited for clinical applications. The resulting stress distributions and values are very similar to the ones returned by the existing iterative methods.

Keywords: Abdominal Aortic Aneurysm; Residual Stress; Finite Element Method; Wall Stress

1. Introduction and motivation

In this report we present an efficient method to include Residual Stress (RS) in patient specific Abdominal Aortic Aneurysm (AAA) wall stress calculations based on the Uniform Stress Hypothesis (USH).

An AAA is the consequence of pathogenic remodelling of the lower aortic wall, resulting in a gradual ballooning and possible rupture. The most common criterion for surgical repair is a diameter exceeding 55 mm. However, the simplicity of this measure masks the complexity of the mechanical environment of real AAAs, and in particular it disregards complex additional factors such as haemodynamics or wall stress state. In practice, correspondingly, it is a relatively poor indicator of rupture likelihood, and can lead to inaccurate and misinformed diagnoses (1). It has been found, for example, that 60% of AAAs with diameters larger than 55 mm do not rupture, while rupture can occur in some AAAs with diameters less than 55 mm (2,3). Conversely, biomechanics-derived criteria, such as Peak Wall Stress and Peak Rupture Risk, may constitute more accurate predictors of AAA rupture (4,5).

RS in arterial walls and its effect on the biomechanical response have been well documented (6–9). It is theorised that it develops as a result of wall remodelling wherein mechanotransducing cells react to applied loads and, through various cell signalling processes, vary wall residual stress through altering protein fibers (commonly elastin and collagen) and increase smooth muscle tone to aid in bearing the circulatory pressure (10). As a result, the RS in healthy arterial walls is most prominent in the circumferential direction, with only a small component in the longitudinal direction. The magnitude of the circumferential RS is commonly measured *ex vivo* using opening angle tests whereby a thin segment of the cylindrical wall is cut longitudinally and the angle is measured, as in Figure 1; larger opening angles thus indicate higher RS (11,12).

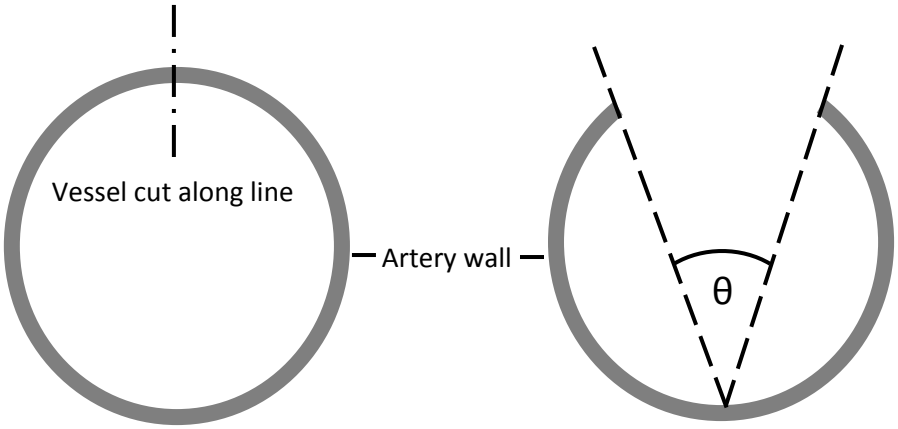

Figure 1. Schematic of cross-section of vessel wall during opening angle experiment. The wall is cut along the dot-dash line and the corresponding angle θ is measured.

RS is an important component of the wall stress distribution. It must therefore be included for wall stress to be an accurate predictor of AAA rupture and, in turn, to replace aneurysm diameter as a criterion for surgical repair. In an AAA, the complicated geometry and corresponding pathogenic remodelling result in a complex RS distribution, which opening angle tests would not accurately capture. In addition, for assessment of AAA rupture in patients, non-invasive measurement of RS is required. To this end, Polzer et al. proposed an algorithm for patient-specific RS estimation based on the assumption that remodelling-derived RS results in an even stress distribution across the vessel wall, according to the Uniform Stress Hypothesis (USH) (13,14). Their algorithm estimates residual strains iteratively for patient-specific AAAs at given times by using a staggered two-field solution approach based on the concept of isotropic volumetric growth. The amount of growth is set such as to minimise the stress difference across the wall. In the present work we propose a new method for calculating RS based on the USH that is considerably less computationally costly, but which achieves similar accuracy to the earlier method. Motivated by the stress distribution found by Polzer et al. for a cylindrical artery (13), we assume that RSs act to evenly distribute bending stresses across the arterial wall thickness. As bending stresses vary asymmetrically, averaging the stress across the wall thickness will create a uniform stress field and account for RS in the process (Figure 2).

In the following, we detail the USH and Polzer et al.'s approach to RS estimation that derives from it. Subsequently, we describe our proposed new approach. We then present our results and compare them to those of Polzer et al. Finally, we discuss the results and associated conclusions.

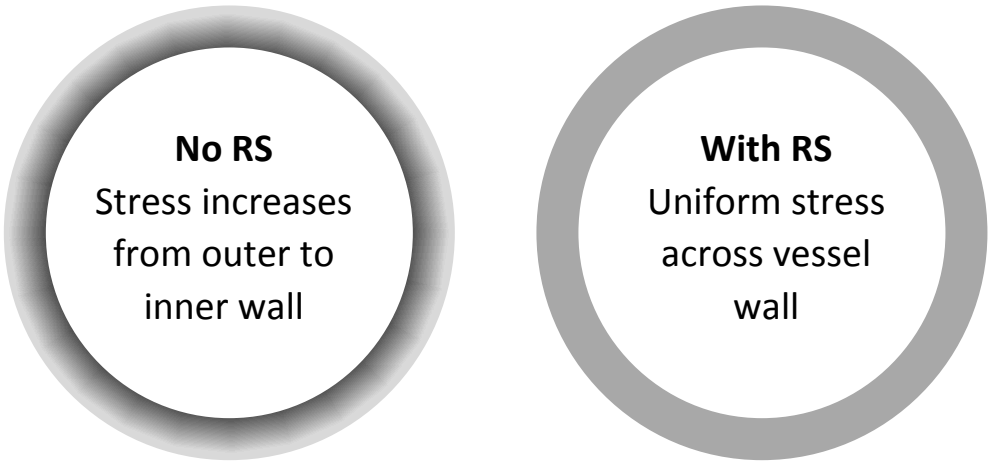

Figure 2. Depiction of the vessel wall without and with RS, according to the uniform stress hypothesis.

2. Methods

2.1. Hypothesis regarding influence of residual stress on the stress distribution in the AAA wall

The uniform stress hypothesis (USH) states that vascular tissue remodels itself toward a preferred stress-strain state, which, in turn, leads to homogenization of stress components across the wall (15). This bears similarities to Wolff's law for bone tissue that states that the structure and density of cancellous bone reflect the loads placed on it (16). Various studies have supported the USH. Lu et al. introduced a unit step change in blood flow in rat femoral arteries to investigate the effect on wall remodeling (17). They found that greater growth in the vessel outer wall compared to in the inner wall resulted in the wall opening angle decreasing, which is consistent with nonuniform remodeling in the USH. Methods similar to those used in opening angle studies have also revealed that circumferential stretches of <1 and >1 exist at the inner and outer arterial surfaces, respectively (6,18,19), similar to the depiction in Figure 1.

2.2. Initial estimation of wall stress

The present study used seven AAA patients that underwent Computer Tomography-Angiography (CT-A) at St. Anne's University Hospital, Brno, Czech Republic, at an in-plane resolution of 0.5 mm and a slice thickness of 3 mm. Deformable (active) contour models (A4research vers.4.0, VASCOPS GmbH, Austria) were used to reconstruct the 3D geometry of AAAs from CT data. After aneurysm segmentation Stereo Lithography (STL) files representing the AAA's geometry (luminal surface, exterior surface, and wall-ILT interface) were exported to ICEM CFD (Ansys Inc., US) for FE mesh generation. The aneurysm wall was meshed with tri-linear hexahedral elements (element type SOLID 185, surface element size of 3mm, four elements across the thickness) while the ILT was meshed with linear tetrahedral elements (element type SOLID 285, element size of 3mm). The very fine ILT mesh aimed at overcoming locking phenomena known from linear tetrahedral elements. The wall thickness was assumed homogeneous with $t = 2mm$. Mesh generation required significant manual interaction and took between four to eight hours for one case. FE meshes were then exported to ANSYS (Ansys Inc., US) for FE computation.

AAA wall mechanical response differs from healthy arterial wall due to the pathogenic remodeling processes altering the density and structure of protein fibers. The AAA wall shows more pronounced strain-stiffening and has reduced anisotropy (20). We therefore utilize an incompressible fifth-order Yeoh strain energy density function to capture AAA wall mean population properties (21):

$$\Psi_{wall} = \sum_{i=1}^{5} c_i (I_1 - 3)^i, \quad (1)$$

with I_1 denoting the first invariant of the right Cauchy-Green deformation tensor and c_i being stress-like material constants **(**Table 1). This model was used previously for modeling AAA rupture risk with RS (14). The AAA intraluminal thrombus (ILT) has a far more linear stress-strain response that was previously captured using an Ogden-like strain energy density function (14), which we used here also:

$$\Psi_{ILT} = \sum_{i=1}^{3} c\left(\lambda_i^4 - 1\right), \quad (2)$$

where λ_i is the i^{th} principal stretch and c is a stress-like material parameter. The ILT is stiffer at the luminal than the abluminal side, which is accounted for in this study using the parameter values in (Table 1) (22).

Table 1. Constitutive parameters used in finite element analysis of AAA wall (5^{th} order Yeoh model) and ILT (Ogden-like model).

Wall (kPa)				
c_1	c_2	c_3	c_4	c_5
5	**0**	**0**	**2200**	**13740**
ILT				
c (Luminal)			c (Abluminal)	
2.62			**1.73**	

The AAA was fixed at the levels of the renal arteries and the aortic bifurcation. The blood pressure was gradually increased up to medium arterial pressure (MAP), while, at the same time, the zero-pressure configuration was predicted, which typically required about 10 iterations.

CT-A modality records the aorta at pulsatile blood pressure, and the images provided, of course, do not reflect AAA zero-pressure geometry which is however required for FE computation. In order to estimate AAA zero-pressure configuration from CT-A-recorded geometry, we used the backward incremental method (23) as modified by (24). Briefly, successive intermediate reference configurations were constructed by subtracting the computed FE-mesh nodal displacements from the previous reference configuration, i.e. until the MAP-loaded model matched the CT-A-recorded geometry.

2.3. Existing method of accounting for the influence of residual stress

Residual stresses can be taken into the account by several approaches. We have slightly improved previously published algorithm which is based on multiplicative decomposition of the deformation gradient tensor:

$$\mathbf{F} = \mathbf{F}_\mathrm{e}\mathbf{F}_\mathrm{g} \tag{3}$$

where $\mathbf{F}_\mathrm{e}$ and $\mathbf{F}_\mathrm{g}$ represent elastic and volumetric growth deformation gradients, respectively. Furthermore, for $\mathbf{F}_\mathrm{g}$ it also holds

$$\mathbf{F}_\mathrm{g} = (1 + \mathrm{c})\mathbf{I}, \tag{4}$$

where c is an engineering-like growth strain which needs to be prescribed in each iteration to minimize stress differences between inner and outer surface. Consequently, the elastic deformation gradient is related to the total deformation gradient $\mathbf{F}$ according to

$$\mathbf{F}_\mathrm{e} = \mathbf{F}\mathbf{F}_\mathrm{g}^{-1} \tag{5}$$

Finally, using standard arguments the Cauchy stress tensor $\boldsymbol{\sigma}$ for hyperelastic and mechanically incompressible materials reads:

$$\boldsymbol{\sigma} = 2\mathbf{F}_\mathbf{e}\frac{\partial \Psi}{\partial \mathbf{C}_\mathrm{e}}\mathbf{F}_\mathrm{e}^\mathrm{T} - p\mathbf{I}\ , \tag{6}$$

where $\mathbf{C}_\mathbf{e} = \mathbf{F}_\mathrm{e}^\mathrm{T}\mathbf{F}_\mathbf{e}$ is the elastic right Cauchy-Green deformation tensor, Ψ is the strain energy density function and p is the hydrostatic stress. For the considered incompressible material, i.e. $J = \det\mathbf{F}_\mathbf{e} = 1$, the hydrostatic pressure is determined by the boundary value problem.

We modified this algorithm as follow: The stress difference in 1st iteration at the k-th node Δ_{1k} is used to estimate the growth deformation at the k-th node according to $c_{2k} = 0.15 \cdot \Delta_{1k}$. The growth deformation at the k-th node in the i-th iteration is now estimated as a linear interpolation of known stress differences resulted from growth prescribed in (i-1) and (i-2) iterations:

$$c_{ik} = c_{(i-1)k} - \frac{c_{(i-2)k} - c_{(i-1)k}}{\Delta_{(i-2)k} - \Delta_{(i-1)k}} \cdot \Delta_{(i-1)k} \tag{7}$$

Using Eq. (7) usually results in faster convergence of the residual stress algorithm. The same mean stress differences can be obtained in average by 2 iterations faster than when original algorithm is used.

2.4. Proposed new method of incorporating the effects of residual stress in the AAA wall stress estimation

The proposed method aims to simplify the above approach by replacing the tissue growth and inverse procedure with a simple single step calculation. Considering the simple wall cross-section shown in Figure 1, in the absence of any RS, the stress along the wall thickness has two components: the hoop stress, created by the hoop forces, and the bending stress, generated by the bending moments. The average bending stress along the wall thickness is zero (as it is created by moments). According to the USH, the stress along the wall thickness is constant due to the inclusion of RS. At the same time, the equilibrium of forces has to be satisfied; therefore the internal wall forces created by this constant stress have to be the same as the hoop forces obtained without the inclusion of RS:

$$\int_{R_1}^{R_2} \bar{\sigma}\,\mathrm{d}r = \int_{R_1}^{R_2} \sigma(r)\,\mathrm{d}r, \tag{8}$$

Therefore, in order to compute the constant stress according to the USH, stresses found through finite element analysis are averaged across the vessel wall according to

$$\bar{\sigma} = \frac{1}{T}\int_{R_1}^{R_2} \sigma(r)\,\mathrm{d}r, \tag{9}$$

where $T = R_2 - R_1$ is the wall thickness and $\sigma(r)$ is the stress component being averaged, which is a function of the radial coordinate r.

With a more complicated 3D geometry, the above equations do not really apply. Nevertheless, under the assumption that the AAA wall is relatively thin, the hoop stress is the main stress occurring in the wall, and the one potentially responsible for the wall rupture. Therefore, we apply Eq. (9) to the maximum principal stress component in order to find the value of the maximum wall stress under the USH.

In order to obtain an accurate value of the average stress, the integral term in Eq. (9) is computed as a sum of piece-wise integrals evaluated on several smaller sub-intervals of the wall thickness, such that

$$\bar{\sigma} = \frac{1}{T}\sum_{k=1}^{n}\int_{M_{k-1}}^{M_k}\sigma(r)\mathrm{d}r, \tag{10}$$

where M_k is the coordinate of the outer boundary of interval k (see Figure 3), and n is the number of sub-intervals. We use equal-sized sub-intervals, meaning their lengths are T/n, and boundary coordinates are given by:

$$M_k = \left(1 - \frac{k}{n}\right)R_1 + \frac{k}{n}R_2. \tag{11}$$

On each sub-interval, a two-point Gauss rule is employed, yielding:

$$\bar{\sigma} \approx \frac{1}{T}\sum_{k=1}^{n}\frac{M_k - M_{k-1}}{2}\sum_{i=1}^{2}\sigma_k^i = \frac{1}{2n}\sum_{k=1}^{n}\sum_{i=1}^{2}\sigma_k^i, \tag{12}$$

where σ_k^i is the stress value at Gauss point i within interval k. Gauss point coordinates in interval k are obtained with standard interval scaling formulae:

$$\begin{aligned} G_k^1 &= (1-t)M_{k-1} + tM_k \\ G_k^2 &= tM_{k-1} + (1-t)M_k \end{aligned} \tag{13}$$

with the position of the points controlled by:

$$t = \frac{1 - \sqrt{\frac{1}{3}}}{2} \tag{14}$$

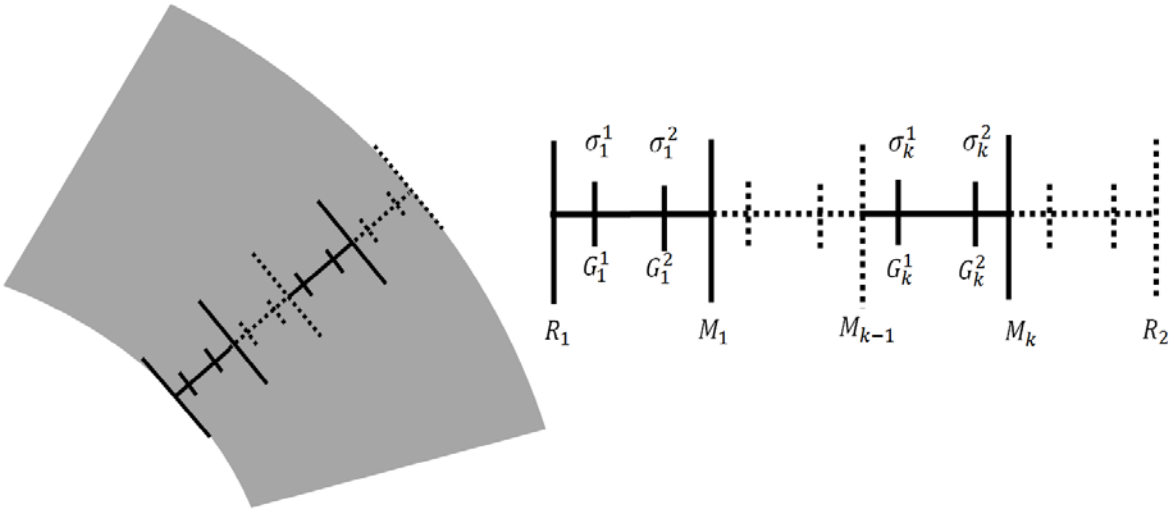

Figure 3. Schematic detailing the Gauss integration procedure to calculate the average stress across the vessel wall. The wall inner radius is given by $\boldsymbol{R_1}$ and the outer radius $\boldsymbol{R_2}$. Sub-interval $\boldsymbol{k}$ is bounded by coordinates $\boldsymbol{M_{k-1}}$ and $\boldsymbol{M_k}$, and $\boldsymbol{\sigma_k^1}$, $\boldsymbol{\sigma_k^2}$ are the stresses interpolated at the Gauss points ($\boldsymbol{G_k^1}$, $\boldsymbol{G_k^2}$) of this sub-interval.

3. Results

We have analyzed 5 cases of AAA with and without the inclusion of residual stresses. The effect of residual stresses has been included using the newly proposed method (Section 2.4), as well as the existing method (Section 2.3). In the new method, we used 4 sub-intervals across the thickness for accurate integration of stress.

The effect of including the residual stress in an AAA analysis using the existing method (Section 2.3) is shown in Figure 4. This method reduces the differences in stress between the interior and exterior walls of the AAA, but does not create a completely uniform stress distribution across the wall thickness.

The newly proposed method assumes a completely uniform stress distribution across the wall thickness. A comparison between the results obtained using the existing method and the proposed method for handling RS is presented in Figure 5. The results show that the new method predicts very similar distributions and levels of stress (Table 2) as the existing method.

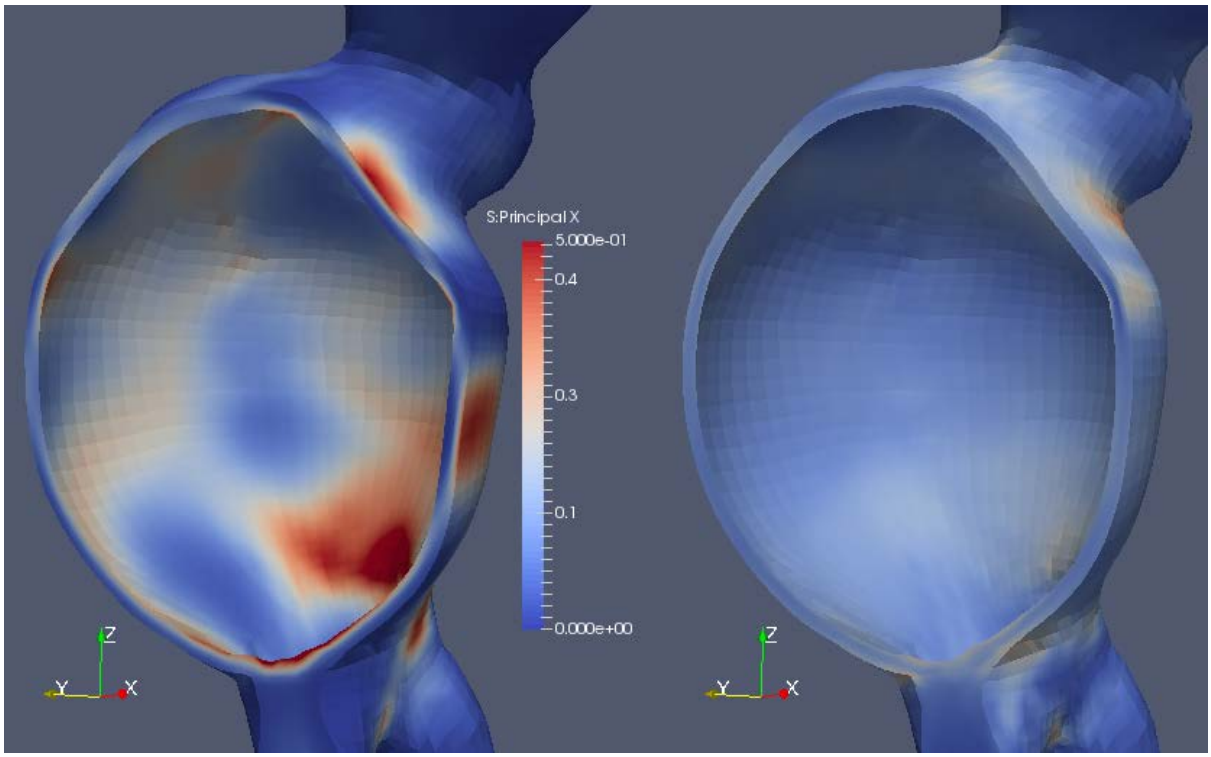

Figure 4. The effect of including the residual stress in an AAA analysis. Maximum principal stress distribution without (left) and with (right) considering residual stress. The residual stress has been included using the existing method described in Section 2.3.

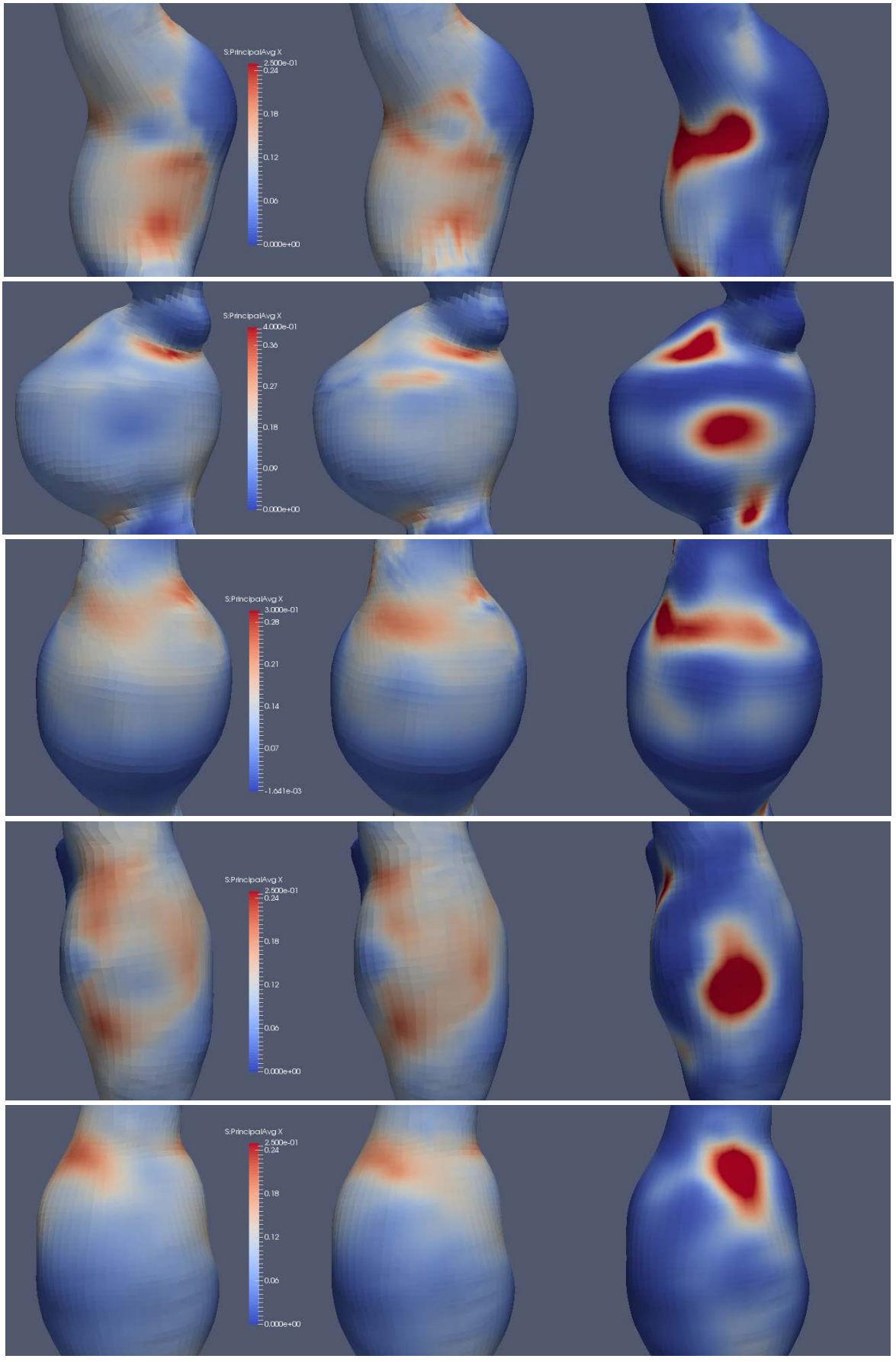

Figure 5. Stress distributions obtained using the new method for RS inclusion (left), the existing method for RS inclusion (middle) and without RS inclusion (right) for 5 cases.

Table 2. Maximum stress values (MPa) obtained using the new method for RS inclusion, the existing method for RS inclusion and without RS inclusion.

Case number	RS inclusion method		
	New method	Existing method	No RS
1	0.22	0.21	0.64
2	0.39	0.39	1.04
3	0.29	0.35	0.69
4	0.21	0.21	0.52
5	0.21	0.19	0.58

4. Discussion and conclusions

By using the Uniform Stress Hypothesis, we developed a new method for including the effects of residual stress in finite element analysis of AAA. The new method requires only the post-processing of a finite element analysis, therefore being very efficient from a computational point of view.

To test the proposed method under the most demanding conditions, we have used in our experiments a highly non-linear material model, which increases the variation of stress across the wall thickness. We have compared the results of using the proposed method against results obtained using an existing iterative method on 5 real geometries of AAA. The newly proposed method predicts similar stress distribution and values for the maximum principal stress, without the computational expense of an iterative method.

The comparative results obtained with and without the inclusion of RS highlight the importance RS inclusion has on both the distribution and value of the wall stress. The inclusion of RS leads not only to a significant reduction in the maximum stress value, but also a different location for the maximum stress areas. Therefore, the inclusion of RS has a great influence on AAA rupture prediction.

Acknowledgements:
This work was partially funded by the 2016 Sheffield International Mobility Scheme and is gratefully acknowledged. We wish to acknowledge the Raine Medical Research Foundation for funding G. R. Joldes through a Raine Priming Grant.

Bibliography:

1. Nicholls SC, Gardner JB, Meissner MH, Johansen KH. Rupture in small abdominal aortic aneurysms. Journal of Vascular Surgery. 1998;28(5):884–8.

2. Heikkinen M, Salenius JP, Auvinen O. Ruptured abdominal aortic aneurysm in a well-defined geographic area. Journal of Vascular Surgery. 2002;36(2):291–6.

3. Darling RC, Messina CR, Brewster DC, Ottinger LW. Autopsy study of unoperated abdominal aortic aneurysms. The case for early resection. Circulation. 1977;56.

4. Gasser TC, Auer M, Labruto F, Swedenborg J, Roy J. Biomechanical rupture risk assessment of abdominal aortic aneurysms: Model complexity versus predictability of finite element simulations. European Journal of Vascular and Endovascular Surgery. Elsevier Ltd; 2010;40(2):176–85.

5. Fillinger MF, Raghavan ML, Marra SP, Cronenwett JL, Kennedy FE. In vivo analysis of mechanical wall stress and abdominal aortic aneurysm rupture risk. Journal of Vascular Surgery. 2002;36(3):589–97.

6. Rachev A, Greenwald S. Residual strains in conduit arteries. Journal of Biomechanics. 2003 May;36(5):661–70.

7. Callaghan FM, Luechinger R, Kurtcuoglu V, Sarikaya H, Poulikakos D, Baumgartner RW. Wall stress of the cervical carotid artery in patients with carotid dissection: a case-control study. American Journal of Physiology. Heart and Circulatory Physiology. 2011 Apr;300(4):H1451–8.

8. Chuong CJ, Fung YC. On Residual Stresses in Arteries. Journal of Biomechanical Engineering. American Society of Mechanical Engineers; 1986;108(2):189–92.

9. Taber LA, Humphrey JD. Stress-Modulated Growth, Residual Stress, and Vascular Heterogeneity. Journal of Biomechanical Engineering. 2001;123(6):528–35.

10. Cardamone L, Valentín A, Eberth JF, Humphrey JD. Origin of axial prestretch and residual stress in arteries. Biomechanics and Modeling in Mechanobiology. 2009;8(6):431–46.

11. Kamenskiy A V, Pipinos II, Dzenis Y a, Lomneth CS, Kazmi SAJ, Phillips NY, et al. Passive biaxial mechanical properties and in vivo axial pre-stretch of the diseased human femoropopliteal and tibial arteries. Acta Biomaterialia. Acta Materialia Inc.; 2014 Mar;10(3):1301–13.

12. Peña JA, Martínez MA, Peña E. Layer-specific residual deformations and uniaxial and biaxial mechanical properties of thoracic porcine aorta. Journal of the Mechanical Behavior of Biomedical Materials. 2015;50:55–69.

13. Polzer S, Bursa J, Gasser TC, Staffa R, Vlachovsky R. A numerical implementation to predict residual strains from the homogeneous stress hypothesis with application to abdominal aortic aneurysms. Annals of Biomedical Engineering. 2013;41(7):1516–27.

14. Polzer S, Gasser TC. Biomechanical rupture risk assessment of abdominal aortic aneurysms based on a novel probabilistic rupture risk index. Journal of The Royal Society Interface. 2015;12(113):20150852.

15. Fung YC. What Are the Residual-Stresses Doing in Our Blood-Vessels. Annals of Biomedical Engineering. 1991;19(3):237–49.

16. Cowin SC. Wolff's law of trabecular architecture at remodeling equilibrium. Journal of Biomechanical Engineering. American Society of Mechanical Engineers; 1986;108(1):83–8.

17. Lu X, Zhao JB, Wang GR, Gregersen H, Kassab GS. Remodeling of the zero-stress state of femoral arteries in response to flow overload. American Journal of Physiology. Heart and Circulatory Physiology. 2001;280(4):H1547–59.

18. Vaishnav RN, Vossoughi J. Residual stress and strain in aortic segments. Journal of Biomechanics. 1987;20(3).

19. Matsumoto T, Hayashi K, Ide K. Residual strain and local strain distributions in the rabbit atherosclerotic aorta. Journal of Biomechanics. 1995;28(10):1207–17.

20. Vande Geest JP, Sacks MS, Vorp DA. The effects of aneurysm on the biaxial mechanical behavior of human abdominal aorta. Journal of Biomechanics. 2006 Jan;39(7):1324–34.

21. Polzer S, Christian Gasser T, Bursa J, Staffa R, Vlachovsky R, Man V, et al. Importance of material model in wall stress prediction in abdominal aortic aneurysms. Medical Engineering and Physics. Institute of Physics and Engineering in Medicine; 2013;35(9):1282–9.

22. Gasser TC, Görgülü G, Folkesson M, Swedenborg J. Failure properties of intraluminal thrombus in abdominal aortic aneurysm under static and pulsating mechanical loads. Journal of Vascular Surgery. 2008;48(1):179–88.

23. De Putter S, Wolters BJBM, Rutten MCM, Breeuwer M, Gerritsen FA, Van de Vosse FN. Patient-specific initial wall stress in abdominal aortic aneurysms with a backward incremental method. Journal of Biomechanics. 2007;40(5):1081–90.

24. Riveros F, Chandra S, Finol EA, Gasser TC, Rodriguez JF. A Pull-Back Algorithm to Determine the Unloaded Vascular Geometry in Anisotropic Hyperelastic AAA Passive Mechanics. Annals of Biomedical Engineering. 2013;41(4):694–708.